

## Proton- $^4\text{He}$ potential derived from phase shifts

S. G. Cooper and R. S. Mackintosh

*Physics Department, The Open University, Milton Keynes, United Kingdom MK7 6AA*

(Received 13 November 1990)

Published phase shifts (in  $R$ -matrix and effective range parametrized forms) fitted to protons scattering from  $^4\text{He}$ , for energies up to 23 MeV, have been inverted to give two alternative energy-dependent local potentials. One is  $l$  independent, the other has a substantial Majorana character; there are very strong reasons to prefer the latter as a potential model for proton scattering from  $^4\text{He}$ . The analysis has novel features: Energy "bites" are introduced as a tool for exploiting the extension of the iterative-perturbative inversion procedure to "mixed-case" inversion for spin-half projectiles. An analysis of  $R$ -matrix parametrized phase shifts for neutrons reveals equal  $n$ - $^4\text{He}$  and  $p$ - $^4\text{He}$  nuclear potentials.

### I. INTRODUCTION

In this paper we establish local potentials which fit the elastic scattering of nucleons from  $^4\text{He}$ . We do not directly fit the differential cross section and spin observables, but apply a phase-shift-to-potential inversion technique to a selection of the many published sets of phase shifts which have been determined by fitting the experimental data. The inversion procedure gives virtually perfect fits to the phase shifts, and so it follows that the potentials we determine fit the observables as well as the fitted phase shifts do; the phase shifts generally fit the data within experimental uncertainties over the range of energies considered. The potentials we find have a very low degree of model or parameter dependence: Any lack of uniqueness in a potential with which we represent a particular set of phase shifts is generally less than the differences between solutions representing different sets of phase shifts fitted to the observables. We can therefore establish that difference between the potentials which corresponds to the difference between alternative phase-shift fits.

The energy range of this study is from near zero to about 23 MeV, the energy of the reaction threshold. As a result,  $S_{lj} = \exp(2i\delta_{lj})$  is unitary, the phase shift  $\delta_{lj}$  is purely real, and the central and spin-orbit potentials are real. The methods we shall describe can readily be applied at higher energies, but for the energy range considered there exist particularly convenient sets of parametrized phase shifts which make a self-contained study. There is indeed interesting physics in the relation between subthreshold and higher-energy scattering, as mentioned in Sec. VII.

The method of analysis involves a number of novel features. The first is the use of "mixed-case" inversion for spin-half scattering. This will be fully described in Sec. III; in brief, it involves arbitrary but generally small sets of partial waves over likewise arbitrary but generally small energy ranges. The other feature is the exploitation of this procedure through "energy bites," permitting us to establish the energy dependence of the potential. The mixed-case inversion procedure is a generalization of the

iterative-perturbative (IP) inversion method,<sup>1</sup> which is an established procedure for fixed energy  $S_{lj}$ -to- $V(r)$  inversion. Mixed-case inversion has previously been applied to spin-zero scattering.<sup>2</sup> For nucleon- $^4\text{He}$  scattering below 23 MeV, in which there are at most four contributing  $l$  values, mixed-case inversion will prove to be the key to extracting significant potentials.

We are fortunate in respect of availability of phase-shifts fits. The proton- $^4\text{He}$  system has, with good reason, been the subject of many experimental and theoretical studies; long ago, the ordering of the low-energy  $P$ -wave resonances helped establish the sign of the nuclear spin-orbit interaction.<sup>3,4</sup> Citations of many of the early experimental and phenomenological papers concerning the  $p$ - $^4\text{He}$  reaction will be found in Arndt, Roper, and Shotwell<sup>5</sup> and Dodder *et al.*<sup>6</sup> More specific references to the analyses exploited by us will be found in Sec. II.

In Sec. III we give an account of mixed-case inversion and briefly review certain technical terms related to IP inversion.

In Sec. IV and V we present evidence for a number of properties of the nucleon- $^4\text{He}$  interaction: (i) The nucleon- $^4\text{He}$  potential is strongly parity dependent, the odd- and even-parity potentials each being radially smooth, but of markedly different radial form; (ii) the energy dependence is rather less than that found by direct potential model fitting of the data; and (iii) the neutron- $^4\text{He}$  and proton- $^4\text{He}$  potentials are identical within the uncertainties of the method.

The first two points suggest that phenomenology based on a phase-shift search followed by inversion may often be superior to direct potential fitting. The published attempt at a direct representation of  $p$ - $^4\text{He}$  data in terms of a potential model<sup>7</sup> yielded what we believe to be a spurious energy dependence. Arguably, parity dependence could not be reliably established by such means in the present circumstances of very few active partial waves.

The third point is particularly striking with respect to the reproduction of the different  $P_{3/2}$  and  $P_{1/2}$  resonance energies for protons and neutrons with nuclear potentials almost indistinguishable graphically.

In Sec. VI we shall discuss the physical significance of

the parity dependence and also the relationship to other work.

## II. R-MATRIX AND EFFECTIVE-RANGE PARAMETRIZED PHASE SHIFTS

Phase shifts determined by fitting observables at a single energy lead to ill-defined potentials owing to the random errors in the phase shifts. Successful parametrizations reproducing the energy dependence of proton-<sup>4</sup>He phase shifts at energies below the reaction threshold exist and are well suited for mixed-case inversion since they enable calculations to be made at any arbitrary energy.

The influence of the  $D_{3/2}$  resonance just above the reaction threshold extends for a couple of MeV below this threshold. A single-channel potential model is an inappropriate model for this resonance, the large partial widths being for  $d + ^3\text{He}$  channels. Just below the threshold,  $S$ -matrix values with the contribution of the  $D_{3/2}$  resonance omitted can be extracted from  $R$ -matrix parametrizations.

Among phase-shift studies below the inelastic threshold, the following have used  $R$ -matrix analyses to provide smooth sets of phase shifts: Stammbach and Walter,<sup>8</sup> Dodder *et al.*,<sup>6</sup> Plattner, Bacher, and Conzett.<sup>9</sup> The representation of  $\delta_{lj}(E)$  below inelastic threshold using effective-range expansions has been effected by Arndt, Roper, and Shotwell<sup>5</sup> and Schwandt, Clegg, and Haeberli.<sup>10</sup> We have also made use of the measurements of Houdayer *et al.*<sup>11</sup>

### A. $R$ -matrix parametrization

All the cited references use the standard theory and notation of Lane and Thomas.<sup>12</sup> There are differences in the way it is implemented, however. Dodder *et al.*<sup>6</sup> use a two-level single-channel  $R$  matrix for  $P$  waves, but a single-level  $R$  matrix for all other partial waves. The boundary-value parameter  $B$  is zero; although this is a natural choice, it means that  $E_\lambda$  is quite different from the actual resonance energies.

Stammbach and Walter<sup>8</sup> took a somewhat different approach. They used a one-level  $R$  matrix for each level, but included a background term  $R^\infty$ :

$$R_{lj} = \frac{\gamma_{lj}^2}{E_{lj}^R - E} + R_{lj}^\infty.$$

Their boundary value parameter  $B$  was chosen to be equal to the shift function evaluated at the level energies,  $B_{lj} = S_l(E_{lj}^R)$ , so that their  $R$ -matrix level energies for  $l = 1$  or  $2$  do correspond to resonance energies.

Parameters for both of these fits had been chosen to fit the phase shifts below 20 MeV. We were interested in looking at as wide a range of energies as possible up to the inelastic threshold, and so we considered how the phase shifts calculated from the above two  $R$ -matrix parametrizations predicted the measurements of Houdayer *et al.*,<sup>11</sup> and Plattner, Bacher, and Conzett<sup>9</sup> between 20 and 23 MeV. It turns out that Stammbach and Walter's fit gave a rather good fit to the higher-energy measurements, but that of Dodder *et al.* was markedly poorer.

For this reason, that part of our studies based on phase shifts derived from  $R$ -matrix parametrizations has been based upon the work of Stammbach and Walter. Their work also conveniently provides similarly parametrized phase shifts for neutron-<sup>4</sup>He scattering so that we have a basis for looking at charge symmetry.

### B. Effective range expansions

In the work of Arndt, Roper, and Shotwell<sup>5</sup> and Schwandt, Clegg, and Haeberli<sup>10</sup> a power-series expansion in energy, with a correction for Coulomb-barrier penetration, is used to give smoothly energy-dependent phase shifts in the energy regions 0–23 and 3–18 MeV for the two data sets, respectively. The  $S$ -wave phase shifts agree well as do the  $P$  waves around the resonances, but the two expansions conflict over the  $D$  and  $F$  waves. The  $D$ - and  $F$ -wave phase shifts are not well determined by the experimental data alone in this energy region, a problem solved by Schwandt, Clegg, and Haeberli by matching them to  $R$ -matrix values above 20 MeV. The  $D_{3/2}$  phase shift above 23 MeV is not predicted correctly, but is not required here. The effective-range phase shifts of Schwandt, Clegg, and Haeberli agree well with the  $R$ -matrix phase shifts of Stammbach and Walter in the lower energy range for all partial waves. The largest discrepancies occur for the energy dependence for  $l = 2$ .

## III. MIXED-CASE INVERSION

### A. A summary of the IP method

Before defining mixed-case inversion, we will first give a brief resume of the IP, iterative-perturbative, inversion procedure. The method was originally introduced<sup>1,13,14</sup> for "fixed energy inversion" (defined in Sec. III B), adapted to spin-zero mixed-case inversion Ref. 2 and herein further generalized to spin-half scattering. Rather than present the method once more, we wish to draw attention to the most essential features of the method which we will refer to in the discussion in later sections. The inversion postulates some "starting potential," the successive modification of which leads to the potential reproducing  $S_{lj}$ . In some cases the starting potential may need to be not too far from the final potential, but may sometimes even be a zero potential. At each iteration, the increment in the potential is some linear combination of the "inversion basis." The quality of fit to the  $S_{lj}$  is quantified by the "phase-shift distance."

An "uncertainty" in the potential may be derived from an error analysis on the sensitivity of the calculated  $S_{lj}$  to the inversion basis. In many cases, as in this paper, the uncertainty is very small, and then, as here, a greater problem can arise through the lack of "uniqueness." The latter relates to the possibility of alternative solutions arising due to the "parameter dependence" of the inversion procedure, i.e., the dependence of the inverted potential upon the starting potential and the size and nature of the inversion basis. The question of uniqueness is particularly important when, as in this paper and despite the

extra information concerning the energy dependence of  $S_{lj}$  used in the mixed-case inversion, the  $S_{lj}$  are fitted with a small inversion basis. In Sec. IV the parameter dependence of the solutions is assessed from inversions using different starting potentials. The sensitivity of the results to the choice of the inversion basis is greatly reduced by the use of singular value decomposition (SVD) matrix technique.<sup>15,16</sup> Questions of both uniqueness and uncertainty have been extensively discussed<sup>1</sup> for IP inversion.

### B. Definition of mixed-case inversion

Generally,  $S_{lj}$ -to- $V(r)$  inversion takes one of two forms: (1) "fixed angular momentum" inversion, the determination of  $V(r)$  that reproduces the phase shift for a single partial wave at all energies, or (2) "fixed energy" inversion, in which "all" partial waves for some energy are represented by a potential. References are listed in Refs. 2 and 17. Of course, in neither case are these ideals possible: In the first case, there is always an upper energy limit and bound state information must be included. In the second case, some matching between partial-wave truncation and radial truncation must be achieved. Mixed-case inversion refers to the intermediate case: the extraction of a potential corresponding to a limited set of partial waves over a limited energy interval. The procedure of extending the IP inversion procedure to the mixed-case form is outlined in Ref. 2 where it is applied to spin-zero scattering of  $\alpha + {}^{12}\text{C}$ .

Of course, fixed angular momentum inversion and fixed energy inversion can now be viewed as particular forms of mixed-case inversion, and Sec. IV A presents an application of the IP inversion algorithm to fixed angular momentum inversion.

For the two standard forms of inversion, the formal inversion procedures (see, for example, Refs. 18 and 17) show by construction that a local and  $l$ -independent potential *exists*, although it may exhibit oscillatory features. However, for arbitrary energy intervals and sets of partial waves, we may have to accept that an approximate fit, or a range of approximate fits, is the best that can be achieved. For example, an extreme case of mixed-case inversion may involve all available partial waves over a wide range of energies. There is no obvious argument that a corresponding local potential exists, and the discovery of such a potential fitting experimental phase shift would be of considerable scientific interest.

### C. Present application of mixed-case inversion

In Ref. 2 mixed-case inversion was applied to derive parity-dependent but essentially energy-independent potentials. In this paper we extend the method to extract the energy dependence of the inverted potentials by the following procedure. We select from the overall energy range a number of small energy intervals, which we call energy "bites," for which we know (or can calculate from a parametrized form as discussed above)  $\delta_{lj}$  at a series of closely spaced energies within each energy bite. The inversion potential for such a set of  $\delta_{lj}$  is considered to be the potential corresponding to the energy at the center of the energy bite. If the inversion is accurate, we then ob-

tain a potential which reproduces the energy dependence of the  $S$  matrix, as well as the mean  $S$ , over that energy interval. Importantly, the extra information corresponding to the energy dependence of the  $S$  matrix allows us to define a potential for a specific energy with considerably less uncertainty.

The use of parametrized phase shifts is now particularly useful in conjunction with inversions from specified energy bites since the size and number of included energy values is under control. In particular, it may be useful to use much smaller energy intervals than would be possible with normal experimental resolution. The size of the energy interval can strongly affect the weighting of different partial waves in the inversion. If the energy dependence of  $\delta_{lj}$  for one partial wave is large, this partial wave may dominate the inversion so that the resulting potential does not accurately fit phase shifts for other partial waves, especially those which are very small. By reducing the size of the energy bite, the importance of the energy dependence of the dominating phase shifts is reduced and the inversion becomes more sensitive to the other phase shifts.

The IP method for mixed-case inversion can also be applied to scattering above threshold to derive a complex potential. Since the imaginary potential is expected to be strongly energy dependent, the inversion must now be confined to small energy bites. A parametrization of the full nonunitary  $S$  matrix is then required.

### D. Evaluation of oscillatory potentials

The existence of practical fixed energy inversion procedures demonstrated that the interesting question is no longer whether there *exists* a local potential which fits elastic-scattering data at some fixed energy (it would seem there always is: that which would be found by inversion), but whether such a potential is smooth or intelligibly oscillatory and dependent upon energy in a regular way. By intelligibly oscillatory, we mean that it has wiggles that can be related to an underlying  $l$  dependence, nonlocality, or identifiable higher-order effects. In mixed-case inversion possible  $l$  dependence can be investigated directly by exploiting the inherent flexibility of the method whereby the inversion may be pursued with various subsets of the partial waves. For example, independent inversion of  $\delta_{lj}$  for odd and even  $l$  furnishes a direct route from empirical  $\delta_{lj}$  to a Majorana character of the potential. Such character would be expected to lead to distinct odd- and even-parity potentials which are less oscillatory than potentials extracted by inverting  $\delta_{lj}$  for all partial waves.

Confronted by oscillatory potentials, however, we must first eliminate those oscillatory features that are an artifact of the inversion procedure. Such features are particularly prevalent in cases where there is a high parameter dependence, as in this paper (see Sec. III A), and the presence of even small potential oscillations at large radii can strongly effect values calculated for the volume integrals and rms radii. To minimize the oscillations we have used the following, somewhat crude, method. Just within the radius at which the potential changes sign, i.e.,

at the onset of the surface oscillations, an exponential tail is fitted to the potential to truncate it to a more physically reasonable range. This may well worsen the fit to the  $\delta_{lj}$  and the inversion procedure must be repeated. Overall, the rate of convergence of the iterations is likely to be considerably reduced and sometimes divergence occurs. However, with careful use of SVD techniques, a much smoother potential can be obtained. In many cases this smoother potential gives a phase-shift distance comparable with that obtained with the highly oscillatory potentials. If surface oscillations are necessary to fit particular features of the  $S$ -matrix behavior, clear convergence will not be obtained following these steps.

#### IV. RESULTS OF CALCULATIONS

Inversion of all  $l$  values over the entire available energy range was not successful, and this is consistent with the theoretical implausibility of such a potential. We are also unable to derive a radially smooth parity-dependent potential, reproducing the entire energy range, of the kind we previously found for  $\alpha$ - $^{12}\text{C}$  scattering.<sup>2</sup> However, mixed-case inversion allows us to represent the parametrized  $S$  matrix in many ways by starting from different subsets of the available  $S$ -matrix data. Three different representations are discussed in the first three subsections below.

We consider  $S$  matrices from both the  $R$ -matrix formulation and from the effective-range expansion. As long as the inversion parameters are held fixed, inversions of alternative parametrized phase shifts then provide a measure of that uncertainty in the potential which is due to the uncertainties in the phase shifts themselves. However, the uniqueness problem can sometimes obscure this analysis, particularly with respect to the spin-orbit potential.

##### A. Fixed angular momentum inversions

Here "fixed angular momentum" inversions entail the incorporation of phase shifts for both values of  $j$  related to the  $l$  in question so that central and spin-orbit potentials are determined together. In general, the inversion of phase shifts for a single  $l$  value over a restricted energy range will not produce a unique potential. In practice, it is easy to find potentials this way, but they are very strongly dependent on the inversion parameters, most noticeably the spin-orbit component. The exception is with  $l=1$ . With the phase shifts of the effective-range parametrization, the low-energy resonances do seem to quite accurately define the potential shape (except for  $r \leq 1$  fm), the volume integrals, and the rms radii. Figure 1 shows two solutions, derived from different starting potentials to fit the  $P$ -wave phase shifts for the energy range 0–17.5 MeV. These solutions reproduce the resonances very accurately. Also shown in Fig. 1 is a similar potential derived to fit the  $R$ -matrix phase shifts. This solution has a larger phase distance, but the agreement between the potentials from the two parametrizations is within the indeterminacy from the parameter dependence. Since only  $P$ -wave potentials can be accurately defined, it is difficult to establish clear systematic differences between poten-

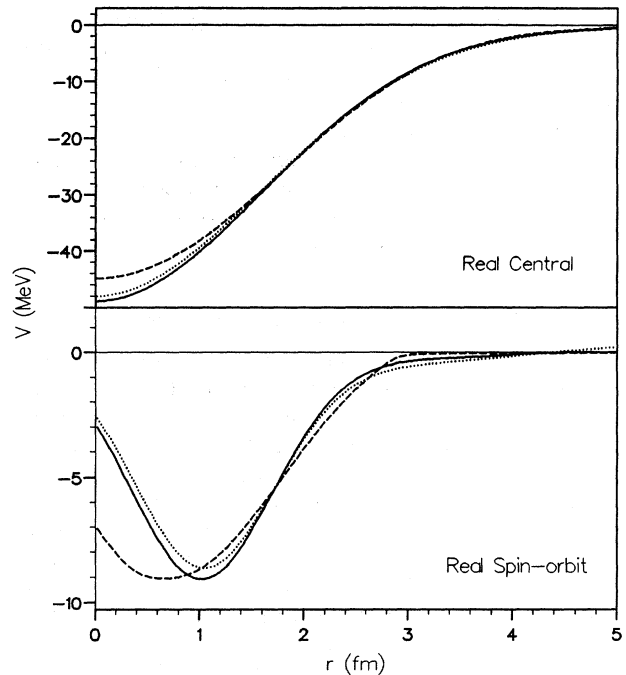


FIG. 1. Inverted potentials fitting the  $P$ -wave phase shifts for  $E=0$ –17.5 MeV from the effective-range parametrization using two different starting potentials (solid and dashed lines) and the  $R$ -matrix parametrization (dotted lines).

tials for different partial waves. We can say, however, that potentials reproducing  $D$ -wave phase shifts, particularly the central components, do not extend as far radially as potentials fitting other partial waves.

##### B. Energy-dependent $l$ -independent potentials

In contrast to the results of the above section, a systematic energy dependence can be obtained by fitting  $\delta_{lj}$  for all partial waves over small energy intervals (bites). Energy bites of  $\pm 0.03$  MeV around a specified energy, with  $\delta_{lj}$  calculated in intervals of 0.01 MeV, were chosen to give reasonable success at the lower energies, around 14 MeV and below. The  $P$ -wave resonances, and in particular the strong energy gradient of these phase shifts compared to small  $D$ - and  $F$ -wave phase shifts, would otherwise dominate the inversion process if much larger energy bites were used. At the higher energies, wider energy bites could be used without significantly affecting the potentials obtained. At still lower energies, 10 MeV and below, the  $D$ - and  $F$ -wave phase shifts become too small to influence the inversion significantly. Hence the predicted values for these  $\delta_{lj}$  may be out by an order of magnitude for potentials essentially derived from  $\delta_{lj}$  for  $l=0,1$  only. In this section we therefore consider only the energy range from 12 to 23 MeV.

All the calculations presented in this subsection have been obtained with at most eight basis functions (after SVD elimination) from which the central and spin-orbit potentials have been derived. In order to be able to

derive volume integrals and rms radii, we have searched for solutions which decay smoothly in the nuclear surface, with minimal surface oscillations, following the procedure outlined in Sec. III D. Examining the parameter dependence of the resulting solutions we find that the potentials are well determined beyond about 1.2 fm, and in particular, the central potential is very well defined between 1.5 and 3 fm. The volume integral and rms radius for the central potential are well determined by the inversion procedure in the following sense: Variations in the values of these quantities due to the parameter dependence of the inversion are less than the differences due to the use of alternative parametrizations of  $\delta_{lj}$ . However, for the spin-orbit potential the volume integral is not well determined and the rms radius varies by up to 10% depending upon the inversion parameters and the particular phase-shift parametrization.

Figure 2 shows the potentials obtained by inversion of the effective-range parametrization for energy bites centered on energies of 12, 16, 20, and 23 MeV. Volume integrals and rms radii for these potentials, and for equivalent calculations from the  $R$ -matrix parametrization, are given in Table I. The scale on the right-hand side of Fig. 2 has been expanded to illustrate an unavoidable problem in these calculations. It has not been found possible to obtain solutions which reproduce the mean values of all phase shifts and which do not contain some degree of oscillations far into the surface. Solutions with a smooth surface behavior can be obtained to simultaneously fit  $l=0, 1$  and  $2$  only and these partial waves determine the basic shape of the potential. The  $D$ -wave phase shifts impose structure in the potential close to the sur-

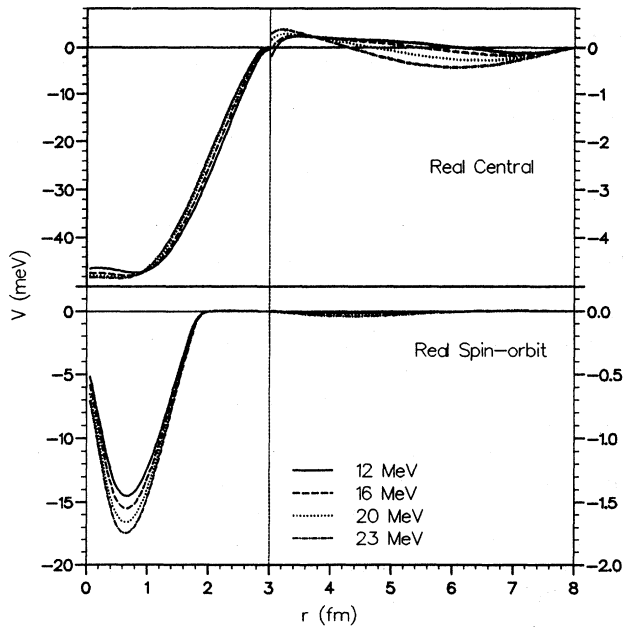


FIG. 2. Potentials obtained by inversion of the effective-range phase shifts, for all  $l$  values and for small energy bites centered around 12 MeV (solid line), 16 MeV (dashed line), 20 MeV (dotted line), and 23 MeV (dot-dashed line).

TABLE I. Volume integrals and rms radii of potentials fitting either the effective-range or  $R$ -matrix parametrized  $S$  matrices for all available  $l$  values for restricted energy bites centered at the specified energies.

Energy (MeV)	Volume integral (MeV fm <sup>3</sup> )		rms radius (fm)	
	Effective range	$R$ matrix	Effective range	$R$ matrix
central potential				
12	517	495	2.18	2.14
16	510	493	2.52	2.55
20	524	517	2.96	3.02
23	553	550	3.32	3.35
spin-orbit potential				
12	43.0	42.3	1.53	1.68
16	47.1	47.5	1.61	1.69
20	51.1	54.9	1.64	1.89
23	53.7	61.1	1.52	2.12

face. A Gaussian-like potential is sufficient to fit the  $S$ - and  $P$ -wave phase shifts alone. To fit all  $l$  values simultaneously, a small oscillation, extending out to at least 8 fm, must be added to the central potential. The form of these oscillations is very dependent on the maximum radius used in the inversion.

All calculations shown in Fig. 2 are made with the same inversion parameters. However, the systematic decrease with energy of the central potential in the nuclear surface is well outside the range of potential variations which would be due to the parameter dependence. Somewhat paradoxically, the volume integral  $J_R$  is almost constant with energy between 12 and 20 MeV, but the rms radius increases from 2.1 to  $\sim 3$  fm within this energy range, due to the long-range oscillations.

Figure 3 displays a set of potentials derived similarly to those in Fig. 2, but from the  $R$ -matrix parametrization of  $\delta_{lj}$ . The central term of these potentials has a somewhat more energy-dependent radial form, but the behavior in the surface is remarkably like that for Fig. 2. Other characteristics are also similar; again, it is clearly evident that the radial extent of the spin-orbit potential is consistently less than that of the central potential. The depth of the spin-orbit potential systematically increases with energy, while the rms radius decreases, although the variation is comparable to the parameter dependence of the solution. However, different fixed sets of inversion parameters each lead to the same energy dependence, and so the energy dependence itself can probably be considered established.

The agreement shown in Table I between the two parametrizations is rather good, including the jump at 23 MeV and the fact that the energy dependence appears to be contrary in sign to both what would be expected and what would appear to be the behavior apparent in Figs. 2 and 3. As suggested above, this surprising result is related to the behavior of the potential in the far surface, which is in itself a particular consequence of fitting the magnitude of the  $F$ -wave phase shifts simultaneously with those of lower  $l$  values.

The potential of Satchler *et al.*,<sup>7</sup> specifically Eq. (8) of

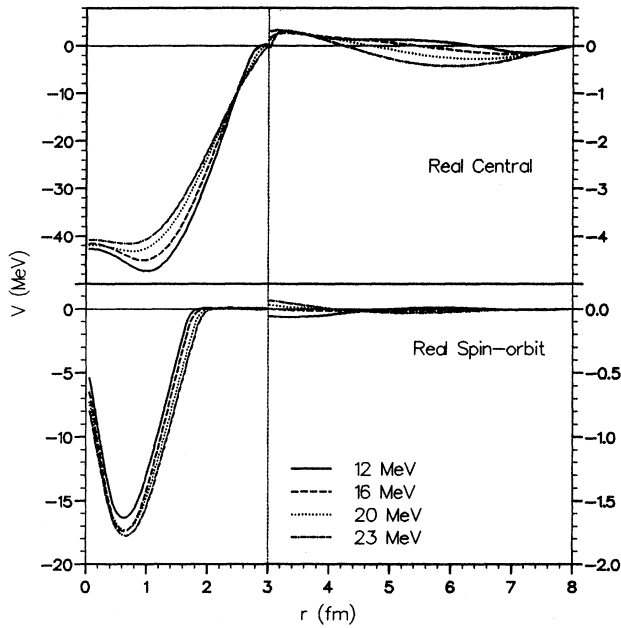


FIG. 3. As for Fig. 2, but showing potentials derived from the  $R$ -matrix phase shifts at the same energy bites.

that work, compares quite closely with the central potentials in Figs. 2 and 3 in the surface region between 2 and 3 fm; the potentials are comparable in magnitude, but the Saxon-Woods shape has the steeper gradient. These differences are not surprising since the latter potential does not fit even the  $D$ -wave phase shifts accurately. The strong energy dependence of  $J_R$  for the potential of Satchler *et al.* is not verified by our calculations and may be an artifact of restricted geometry.

### C. Parity-dependent potential

We have previously shown<sup>19</sup> that inverting the  $S$  matrix derived from an explicitly parity-dependent potential leads to an  $l$ -independent potential of very strongly oscillatory character. The unavoidable long-range surface oscillations in the potentials of Sec. IV B suggest that there may be some form of underlying  $l$  dependence. Given only four values of  $l$ , a parity-dependent potential is the only reasonable form of  $l$  dependence. Using the same energy bites as above, we can find potentials which fit either all-odd- or all-even- $l$  phase shifts for energies down to  $\sim 12$  MeV, below which the  $F$ -wave phase shifts are too small. The size of the energy bite is more crucial for the odd- $l$  values than for the even- $l$  values.

Figure 4 shows potentials calculated at 12 and 20 MeV, which reproduce either the even- or odd- $l$  phase shifts of the effective-range theory. These potentials are much smoother than those in Fig. 2, having no surface oscillations, and very accurately fit the relevant phase shifts. Since these potentials are now obtained with even fewer basis functions than in Sec. IV B, a larger parameter dependence may be expected, particularly with respect to the spin-orbit potential determined entirely by the small

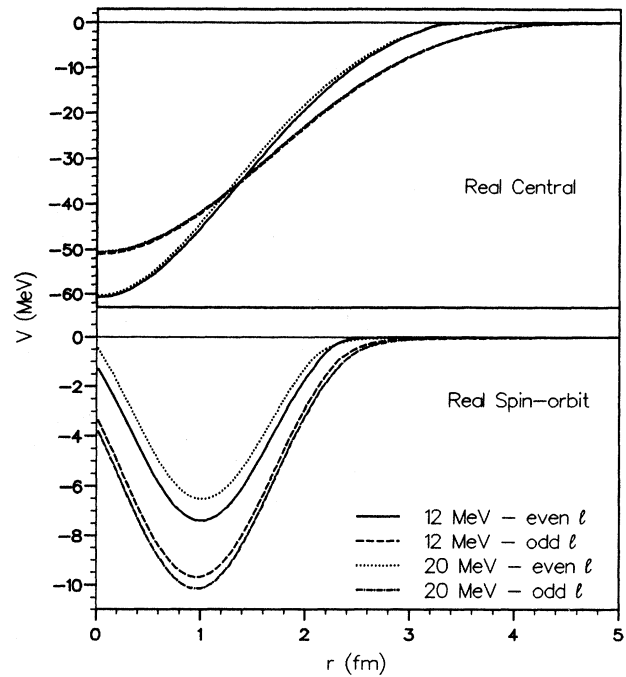


FIG. 4. Parity-dependent potentials fitting the effective-range phase shifts for energy bites centered at 12 MeV, for even  $l$  only (solid line) and odd  $l$  only (dashed line), and 20 MeV for even  $l$  (dotted line) and odd  $l$  (dot-dashed line). The odd-parity central potentials for the two energies are barely distinguishable in this figure.

$D$ -wave phase shifts. For the even spin-orbit potential, both the volume integral and rms radius depend very heavily on the starting potential. The central potentials, however, appear generally rather well determined, unless the potentials of Fig. 2 are used as the starting potential. Since the latter potentials fit all  $\delta_{lj}$  with  $l \leq 2$ , they must also fit the even- $l$  phase shifts only. They can be thought of as the appropriate even- $l$  potential of Fig. 4, but having an additional oscillation, necessary to fit  $l=1$ , and therefore a superfluous feature in a solution to fit  $\delta_{lj}$  for even  $l$  only. The potentials shown in Fig. 4 are probably very close to the smoothest solutions fitting the required phase shifts.

We see from Fig. 4 that considering the odd or even  $\delta_{lj}$  alone leads to central potentials having distinctly different shapes. The even- $l$  central potential must be deeper at the center, but the odd potential extends further in radial range; this is apparently the case for the spin-orbit term too. Unsurprisingly, the odd- $l$  potential is very close to the potential derived in Sec. IV A to fit the  $P$ -wave resonances and the most significant difference appears in the nuclear surface where the potentials of Fig. 4 have a slightly reduced radial extent. The energy dependence apparent in Fig. 4 is much less than for the potentials in Fig. 2 for both the odd- $l$  and even- $l$  potentials. The 16-MeV potential, not shown, agrees well with those illustrated. The discernible systematics mirror the energy dependence of Fig. 2, but on a much smaller scale. The energy dependence of the  $l$ -independent potentials might

simply be a manifestation of the importance of different partial waves at different energies.

Calculating corresponding parity-dependent potentials from  $R$ -matrix phase shifts, we find potentials which agree with the effective-range potentials to much the same extent that Fig. 3 agrees with Fig. 2. The agreement between effective-range and  $R$ -matrix potentials is very good in the surface, but there are differences for  $r$  less than about 1.3 fm. However, there is a somewhat greater energy dependence in the even potential than there is in Fig. 4 for the effective-range even- $l$  potential.

In Table II we present the volume integrals and rms radii for the parity-dependent potential fitting  $\delta_{lj}$  from the effective-range parametrization. It will be seen that the real volume integral  $J_R$  falls rather slowly with energy. It is interesting that  $J_R$  in Table I rises, although quite slowly between 12 and 20 MeV, in spite of the apparently conspicuous greater energy dependence of the  $l$ -independent potential, apparently in the direction of a fall with energy. The resolution of this apparent paradox lies in the observation that for the  $l$ -independent potential, the calculation of  $J_R$  gets a large contribution from the far surface.

#### D. Comparison of different representations

Setting aside, for reasons of the large parameter dependence, the solutions of Sec. IV A, we effectively have two alternative means of fitting  $\delta_{lj}$ : (i) an  $l$ -independent potential, appreciably energy dependent in form and having a surface structure extending to a radius well beyond what would be expected for nuclear forces, or (ii) a parity-dependent potential, which is much less energy dependent in shape, is both smoother and less extended in the surface and which actually gives better fits to  $\delta_{lj}$  as measured by the phase-shift distance.

It is also to be noted that the energy dependence of  $J_R$  for the parity-dependent potential is in the "correct" sense, falling with energy.  $J_R$  for the  $l$ -independent potential increases with energy.

The presence of long-range oscillations, extending beyond the range of any probable nuclear force, is a legitimate reason for rejecting a potential. The significance of the potential found in Sec. IV B lies precisely in the

demonstration that a local and  $l$ -independent potential that fits the phase shifts has unphysical properties. From Secs. IV B and IV C taken together, we conclude that the  $\delta_{lj}$  fitted to experiment carry the implication that a local potential model of proton-<sup>4</sup>He scattering must contain a substantial Majorana term. This could not be deduced from the tabulated phase shifts. Direct potential fits involving parametrized Majorana terms have never been convincing for proton scattering.<sup>20</sup>

What is the significance of the difference between these potentials? They will have correspondingly different scattering wave functions and these differences could therefore produce very different results when used in reaction calculations. In a microscopic study of  $p + ^4\text{He}$  bremsstrahlung, Liu, Tang, and Kanada<sup>21</sup> were able to give a good reproduction of the experimental data using nonlocal wave functions derived from resonating-group theory. Wave functions which are only asymptotically equivalent may not be as successful. We are unable to repeat their calculations here, but for any given energy we can calculate and compare the full scattering wave functions (summed over all partial waves) obtained from the potentials calculated in the previous sections.

We have two potentials reproducing certain phase shifts, one  $l$  dependent and one  $l$  independent, and they lead to the same wave functions in the asymptotic region. To compare them we plot the "generalized Perey factor"  $R(r, \theta, \phi)$  defined following Ref. 22 (where nonlocality rather than  $l$  dependence was the issue) as

$$R(r, \theta, \phi) = \frac{|\psi_{l-\text{dep}}(\mathbf{r})|}{|\psi_{l-\text{indep}}(\mathbf{r})|} \quad (1)$$

In Fig. 5 we present  $R(r, \theta, \phi)$  at 20 MeV for potentials fitting effective-range phase shifts. Thus  $|\psi(\mathbf{r})|$  is calculated with the appropriate parity-dependent potential of Fig. 4 and divided by  $|\psi(\mathbf{r})|$  calculated with the corresponding potential from Fig. 2. The dominant feature is the large decrease, up to 50%, around 1–2 fm, of the wave function due to the parity-dependent potential compared with its  $l$ -independent equivalent. The largest differences between the wave functions in percentage terms occur in radial regions where the wave functions are small, notably the regions where  $R(r, \theta, \phi) > 1$ . In the region behind the nucleus, the wave functions have a large focus and here the difference between the two wave functions is still over 15%. At the lower energy of 12 MeV, the effect is even stronger in the radial regions where the wave function is largest, principally at the focus in the backward direction.

The asymmetry of  $R(r, \theta, \phi)$  about the line of zero impact parameter is due to the spin-orbit potential, as discussed in Ref. 22. The fact that  $R$  is not exactly unity at the edge of the diagram is due to the extended tail of the  $l$ -independent potential.

The behavior of  $R(r, \theta, \phi)$  is not affected by the range of variation in the potentials arising from the parameter dependence, discussed above, inherent in the inversion procedure. Furthermore, an equivalent calculation of  $R(r, \theta, \phi)$  using potentials fitting the  $R$ -matrix  $\delta_{lj}$  gives a contour plot only very slightly different to Fig. 5.

TABLE II. Volume integrals and rms radii of parity-dependent potentials which fit the effective-range parametrized  $\delta_{lj}$  in energy bites centered at the specified energies. An asterisk denotes a quantity with large parameter dependence.

Energy (MeV)	Volume integral (MeV fm <sup>3</sup> )		rms radius (fm)	
	even $l$	odd $l$	even $l$	odd $l$
	central potential			
12	450	679	1.94	2.41
16	438	672	1.94	2.41
20	430	673	1.94	2.42
	spin-orbit potential			
12	43.7*	69.2	1.53*	1.77
16	41.1*	72.5	1.60*	1.77
20	39.0*	75.0	1.70*	1.77



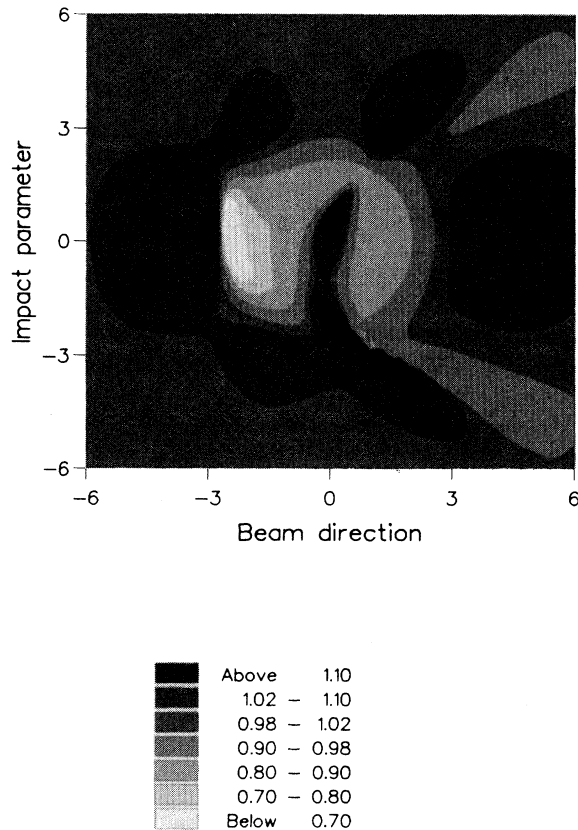


FIG. 5. A contour plot of  $R(r, \theta, \phi)$  in the plane with  $\phi=0$  or  $\pi$  for 20 MeV, comparing the wave function calculated with the parity-dependent potential of Fig. 4 with that from the  $l$ -independent potential of Fig. 2.

### V. CHARGE SYMMETRY OF THE NUCLEON- $^4\text{He}$ INTERACTION

The  $R$ -matrix fit to  $n$ - $^4\text{He}$  scattering of Stambach and Walter enables us to perform a similar set of inversion calculations to those made above for  $p$ - $^4\text{He}$  scattering. Within the degree of numerical uncertainties discussed in preceding sections, a close agreement was found between the proton and neutron potentials. Consider, for example, the energy-independent inversion of the  $P$ -wave phase shifts only. Figure 6, closely analogous to Fig. 1, shows potentials derived from fitting the  $P$ -wave phase shifts only, for  $E=0$ –17.5 MeV as before, for either the  $p$ - $^4\text{He}$   $R$ -matrix parametrization (full line) or for the  $n$ - $^4\text{He}$   $R$ -matrix parametrization (dashed line). Both potentials accurately reproduce the shapes of the  $P$ -wave resonances, whose energies differ due to the presence or absence of the Coulomb force. The agreement between the potentials in Fig. 6 is well within variations expected from the inversion parameter dependence (cf. Fig. 1) and constitutes a textbook example of charge symmetry.

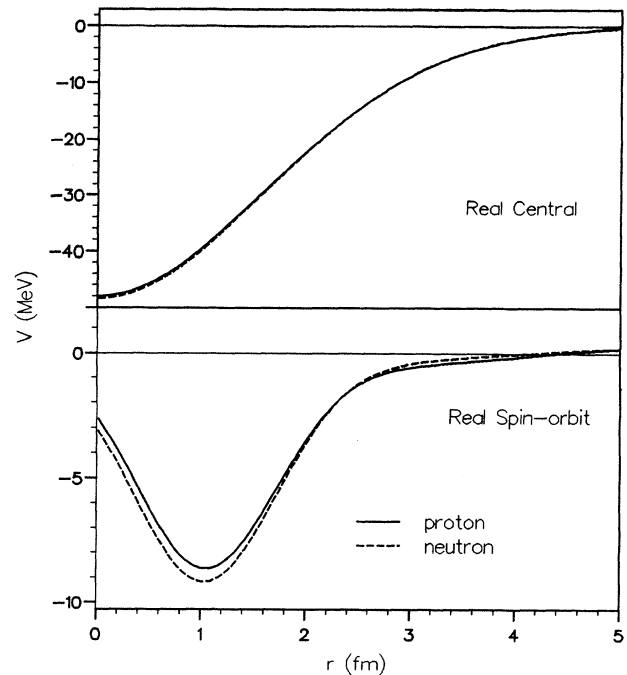


FIG. 6. As for Fig. 1, comparing the potential derived to fit the  $p$ - $^4\text{He}$   $R$ -matrix  $P$ -wave phase shifts with that derived for  $n$ - $^4\text{He}$  scattering.

The results of Secs. IV B and IV C can also be closely reproduced with potentials fitting the  $n$ - $^4\text{He}$  system. Potentials derived to fit the same energy bites as in Sec. IV B can only reproduce all partial waves if long-range radial oscillations are introduced, which very closely resemble the form of those needed to fit the  $p$ - $^4\text{He}$   $R$ -matrix phase shifts. For all but the innermost radial region, the central potential is more narrowly determined by the energy of the calculation than by the choice of projectile. The spin-orbit potential is not very well determined for the  $R$ -matrix neutron scattering, but for fixed inversion parameters a steady decrease in the potential depth is found.

Smooth potentials can again be obtained if only either even- $l$  or odd- $l$  partial waves are fitted. Figure 7 compares, for 20 MeV laboratory energy, the parity-dependent potential fitting the proton  $R$ -matrix  $\delta_{lj}$  with that fitting the neutron  $\delta_{lj}$ . The agreement between the potentials fitting odd  $l$  is most striking, and a similar agreement is found at other energies. For the even- $l$  case agreement between the two projectiles is found mainly in the surface region, but the energy dependence of these potentials is very similar. A plot of  $R(r, \theta, \phi)$  relating the neutron  $l$ -independent and parity-dependent potentials at 20 MeV reveals characteristics very close to those displayed in Fig. 5. The minor differences between contours of  $R(r, \theta, \phi)$  for protons and neutrons are no more significant than the differences between the contours for protons derived from  $R$ -matrix or effective-range phase shifts.



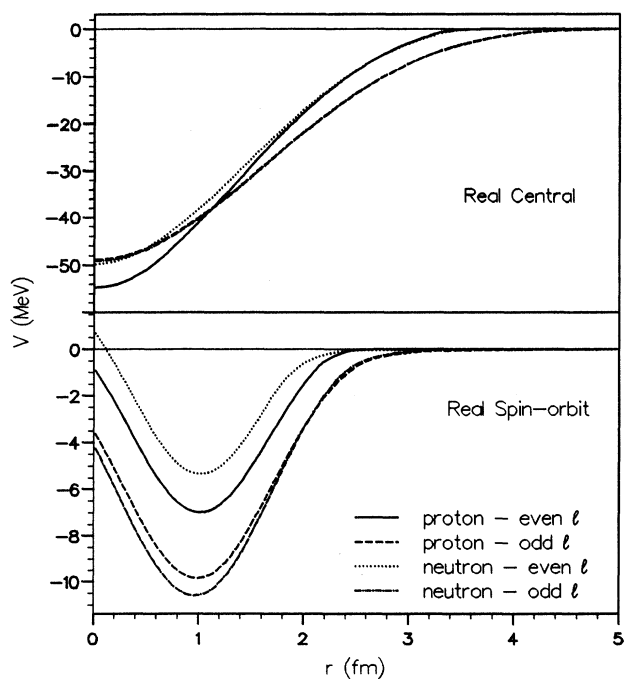


FIG. 7. For energy bites centered at 20 MeV, potentials fitting either even- or -odd- $l$  values only for  $p + {}^4\text{He}$  (solid and dashed lines, respectively) and corresponding potentials for  $n + {}^4\text{He}$  scattering (dotted and dashed lines, respectively). The odd-parity central potentials for the two projectiles are barely distinguishable in this figure.

## VI. RELATION TO OTHER WORK

The preferred optical potential of Satchler *et al.*<sup>7</sup> exhibits a volume integral which falls from 674 MeV fm<sup>3</sup> at 0 MeV to 453 MeV fm<sup>3</sup> at 20 MeV. This change reflects a radius parameter which diminishes linearly with energy. If this trend were followed to higher energies, the potential would rapidly become unphysically shallow; it is clear that the potential in question is much too energy dependent. The potential “closely reproduces the observed scattering” in the customary sense of these words. We find very much less energy-dependent volume integrals, but the irreducible surface features in our potentials makes comparisons based on volume integrals open to question. The  $l$ -independent potentials of Sec. IV B do exhibit a decrease in radius with energy. However, as noted in Sec. IV D, we prefer a parity-dependent model. The  $D$  and  $F$  waves played a vital role in establishing this model, and these phase shifts are not fitted by the potential of Satchler *et al.*

Resonating-group calculations suggest some degree of parity dependence, (cf. Fig. 3 of Shen and Tang<sup>23</sup>), which can be traced to exchange processes. In particular, Shen and Tang demonstrate the importance of recoil effects in calculations of the phase shifts. The staggering visible in their Fig. 3, possibly to be construed as parity dependence, appears to be an effect of the inclusion of recoil. This is interesting, since the other recent theoretical cal-

culations, due to Lassaut and Vinh Mau<sup>24</sup> (see also Sofianos *et al.*<sup>25</sup>) are effectively a folding model with a Fock term for exchange, the nuclear structure being expressed as independent particles in a harmonic oscillator. Such models are, of course, standard for heavier nuclei, and it is clearly important to demarcate the mass regime where full treatments of recoil and center-of-mass effects are obligatory. The Lassaut and Vinh Mau nonlocal potentials have been expressed as local  $l$ -independent equivalent local potentials by Sofianos *et al.* It does seem that for the mass-5 system a proper treatment of recoil and related effects is necessary, and that their neglect is related to a failure to predict parity dependence.

The existence of parity dependence has further significance since it may be related to one of the conspicuous features of nucleon-<sup>4</sup>He scattering at energies above the reaction threshold. There the absorption is predominantly in the positive-parity partial waves;<sup>9</sup> causality implies that this must have consequences for the real potential below threshold. As a consequence, one must suppose some connection between the predominance of absorption at higher energies and exchange processes.

We must address the relationship of our present work to our earlier inversion work on the proton-<sup>4</sup>He scattering<sup>26</sup> at about 65 MeV. There fixed energy inversion was applied to a large number of partial waves and an  $l$ -independent potential was determined. However, in that paper we concluded from the presence of oscillatory structure that the  $l$ -independent potential presented there is “almost certainly an  $l$ -independent equivalent of a more fundamental potential having a substantial degree of  $l$  dependence.” It does appear that some or all of that  $l$  dependence is of Majorana (parity-dependent) character. It would appear that our present study does not imply a rapid falloff of Majorana character with energy.

## VII. SUMMARY AND CONCLUSIONS

In this paper we have introduced a new methodology and obtained specific results concerning the nucleon-<sup>4</sup>He potential. These results raise various questions relating to scattering phenomenology and experiment and also relating to nuclear theory.

*The nucleon-<sup>4</sup>He potential.* We have found alternative potentials which, insofar as the corresponding phase shifts fit the experimental data, give precise fits to the proton-<sup>4</sup>He scattering data at energies below the reaction threshold. Applying reasonable criteria to these potentials, we conclude that the nucleon-<sup>4</sup>He potential has a substantial Majorana component at these energies. The odd- and even-parity potentials have different forms as well as different depths.

The existence of  $R$ -matrix fits for both neutrons and protons scattering from <sup>4</sup>He over the same energy range enabled us to show that, to within the accuracy within which these parametrized  $\delta_{lj}$  fitted the empirical data, the neutron-<sup>4</sup>He and proton-<sup>4</sup>He nuclear potentials were the same. The convergence between the potentials found with  $R$ -matrix and effective-range  $\delta_{lj}$  for protons as well as  $R$ -matrix  $\delta_{lj}$  for protons and neutrons lends a degree

of confidence to our results. The neutron and proton  $\delta_{lj}$  are sufficiently unlike for the final potential shapes, which are essentially the same, to be an artifact of the inversion process. Of course, we have also checked for "parameter dependence" at every stage of the inversions.

*Methodology.* Our analysis has two novel elements: (i) the use for the first time of spin-half mixed-case inversion and (ii) the use of energy bites to exploit the former, and introduce information relating to the energy dependence of  $\delta_{lj}$  into the inversion. A prerequisite was the existence of parametrized phase-shift fits to the data. The  $R$ -matrix  $\delta_{lj}$  gave generally similar results to  $\delta_{lj}$  from high-order effective-range parametrizations. Energy-by-energy phase-shift fitting, especially with incomplete data, suffers large highly correlated uncertainties. The consequence is that the character of the phase-shift solution can change randomly with energy, undermining the inversion procedure.

Concerning mixed-case inversion, it is likely to be of quite wide interest in nuclear physics because one cannot impose *a priori* the assumption of energy independence upon any nucleon-nucleus potential. This makes the "Gel'fand Levitan" (one partial wave—all energies) type of inversion unrealistic in general. However, one supposes that there should always be energy bites which are at once wide enough to contribute information to the inversion, but narrow enough for a potential to be defined for that bite.

*Implications for phenomenology and experiment.* We believe that neither the charge symmetry nor the parity dependence could have been extracted reliably from the empirical data by other means. Certainly, neither property is any way apparent by inspection of the  $\delta_{lj}$ .

We suggest that there are many circumstances where the method of choice for fitting elastic-scattering data by a potential model is to fit  $S_{lj}$  and follow this with inversion. At best, the so-called model-independent fitting procedures would have led in the present case only as far as the oscillatory potentials, which we were able to supercede with parity-dependent potentials. A key feature of

the present method is that it permits the use of physically well-grounded extrapolation methods to establish phase shifts at energies where they would otherwise be empirically ill determined. In addition, at the inversion step at least, the two-step method gives considerable scope for having control over both uncertainties and nonuniqueness (alternative solutions outside the error bands corresponding to uncertainties). This latter may be more prevalent in model-independent fitting than often supposed, and many published error bands may be subject to reevaluation as representing local minima. This conclusion follows from a consideration of the ambiguities found in phase-shift fitting with even the most complete available sets of observables.

Any advance in the phenomenology in the scattering of nucleons on He at low energies must await measurements of spin rotation parameters. That this could be worthwhile is suggested by the fact that one of the new precise fits to nucleon-nucleus scattering including a fit to spin rotation observables, and involving a wide angular range for all observables, reveals a potential with certain unexpected properties (see Ref. 26).

*Implications for nuclear theory.* It is possible that the Majorana potential below the inelastic threshold could be linked by causality considerations to the markedly greater absorption in positive-parity channels, which is a conspicuous aspect of the  $S_{lj}$  above the inelastic threshold.<sup>9</sup>

The parity dependence of the interaction raises interesting questions since the even channel absorption above threshold is generally attributed to broad even-parity resonances and the source of parity dependence in resonating-group calculations is exchange processes. The challenge is to lay bare the underlying relationship between these two effects.

We are grateful to Prof. Y. C. Tang for helpful comments and to the Science and Engineering Research Council of the U.K. for Grant No. GR/F12501 supporting S. G. Cooper.

<sup>1</sup>S. G. Cooper and R. S. Mackintosh, *Inverse Problems* **5**, 707 (1989).

<sup>2</sup>S. G. Cooper and R. S. Mackintosh, *Nucl. Phys.* **A517**, 285 (1990).

<sup>3</sup>C. L. Critchfield and D. C. Dodder, *Phys. Rev.* **76**, 602 (1949).

<sup>4</sup>M. Heusinkfeld and G. Freier, *Phys. Rev.* **85**, 80 (1952).

<sup>5</sup>R. A. Arndt, L. D. Roper, and R. L. Shotwell, *Phys. Rev. C* **3**, 2100 (1971).

<sup>6</sup>D. C. Dodder, G. M. Hale, N. Jarmie, P. W. Keaton, R. A. Nisley, and K. Witte, *Phys. Rev. C* **15**, 518 (1977).

<sup>7</sup>G. R. Satchler, L. W. Owen, A. J. Elwyn, G. L. Morgan, and R. L. Walter, *Nucl. Phys.* **A112**, 1 (1968).

<sup>8</sup>Th. Stammbach and R. L. Walter, *Nucl. Phys.* **A180**, 225 (1972).

<sup>9</sup>G. R. Plattner, A. D. Bacher, and H. E. Conzett, *Phys. Rev. C* **5**, 1158 (1972).

<sup>10</sup>P. Schwandt, T. B. Clegg, and W. Haeberli, *Nucl. Phys.* **A163**,

432 (1971).

<sup>11</sup>A. Houdayer, N. E. Davison, S. A. Elbaker, A. M. Sourkes, W. T. H. van Oers, and A. D. Bacher, *Phys. Rev. C* **18**, 1985 (1978).

<sup>12</sup>A. M. Lane and R. G. Thomas, *Rev. Mod. Phys.* **30**, 257 (1958).

<sup>13</sup>R. S. Mackintosh and A. M. Kobos, *Phys. Lett.* **116B**, 95 (1982).

<sup>14</sup>A. A. Ioannides and R. S. Mackintosh, *Nucl. Phys.* **A467**, 482 (1987).

<sup>15</sup>W. H. Press, B. P. Flannery, S. A. Teukolsky, and W. T. Vetterling, *Numerical Recipes* (Cambridge University Press, Cambridge, England, 1986).

<sup>16</sup>S. G. Cooper and R. S. Mackintosh, *Nucl. Phys.* **A513**, 373 (1990).

<sup>17</sup>K. Chadan and P. C. Sabatier, *Inverse Problems in Quantum Scattering Theory*, second ed. (Springer-Verlag, New York,

- 1989).
- <sup>18</sup>M. Münchow and W. Scheid, *Phys. Rev. Lett.* **44**, 1299 (1980).
- <sup>19</sup>S. G. Cooper and R. S. Mackintosh, *Z. Phys. A* **337**, 357 (1990).
- <sup>20</sup>F. K. Vosniakos, N. E. Davison, W. R. Falk, O. Abou-Zeid, and S. P. Kwan, *Nucl. Phys.* **A332**, 157 (1979).
- <sup>21</sup>Q. K. K. Liu, Y. C. Tang, and H. Kanada, *Contributions to the International Symposium on Nuclear Astrophysics*, June, 1990, Baden/Vienna.
- <sup>22</sup>S. G. Cooper and R. S. Mackintosh, *Nucl. Phys.* **A511**, 29 (1990).
- <sup>23</sup>P. N. Shen and Y. C. Tang, *Phys. Rev. C* **6**, 1985 (1987).
- <sup>24</sup>M. Lassaut and N. Vinh Mau, *Phys. Lett.* **70B**, 14 (1977).
- <sup>25</sup>S. A. Sofianos, H. Fiedeldey, L. J. Allen, and R. Lipperheide, *Phys. Rev. C* **31**, 2300 (1985).
- <sup>26</sup>S. G. Cooper and R. S. Mackintosh, *Phys. Rev. C* **40**, 502 (1989).

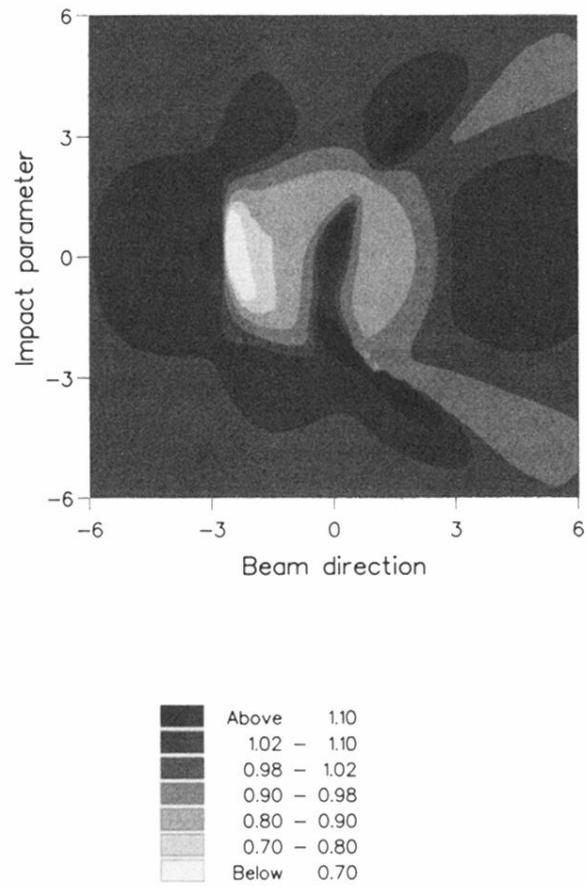


FIG. 5. A contour plot of  $R(r, \theta, \phi)$  in the plane with  $\phi=0$  or  $\pi$  for 20 MeV, comparing the wave function calculated with the parity-dependent potential of Fig. 4 with that from the  $l$ -independent potential of Fig. 2.